geosciences

MDPI

Article

# Universal Shapes? Analysis of the Shape of Antarctic Tafoni

**Rob Inkpen [1] and Kevin Hall [2,*]**

[1] Department of Geography, University of Portsmouth, Buckingham Building, Lion Terrace, Portsmouth and Hampshire PO1 3HE, UK; robert.inkpen@port.ac.uk
[2] Department of Geography, Rhodes University, Grahamstown 6139, South Africa
* Correspondence: Kevin.Hall@unbc.ca

Received: 11 February 2019; Accepted: 25 March 2019; Published: 2 April 2019


**Abstract:** Using dimensional data from over 700 tafoni in Antarctica, this paper identifies how the dimensionless ratios of width/length (W/L) and depth/length (D/L) vary with tafoni length. The analysis suggests that these ratios do tend to converge to values that are similar to those found for fragments produced by brittle fracture and fragmentation. Dividing the data into quintiles and deciles, it is possible to assess how tafoni size and shape change as tafoni length increases. Smaller tafoni do tend to have a rounder plan form which rapidly changes as tafoni length increases towards the W/L ratio of 0.67. It is suggested that initial tafoni development is limited by the conditions set out in a recent mathematical model of tafoni development. This model focuses on tafoni development through the interactions of variable rock strength and the varying concentration gradient of a corrosive agent. Erosion involves the removal of relatively small sections of rock and is analogous to a continuous erosional process. This model produces tafoni of relatively circular plan form. Above a certain tafoni length it is suggested that processes associated with brittle fracture begin to dominant the development and shape of tafoni.

**Keywords:** tafoni modelling; brittle fracture; fragmentation; ratios

## 1. Introduction

Despite a long history of academic study [1–4] there remain ongoing debates about the nature and definitions of tafoni or as these forms have been alternatively called, sometimes within the same paper, alveolar weathering, honeycomb weathering or cavernous weathering [5–13]. Identification and often quantification of hollows in rock surfaces of varying dimensions that occur singularly, and as regularly-spaced swarms have formed the basis of a range of inferred processes of formation Figures 1 and 2 illustrates the forms that are the focus of this particular paper. The different terminology maybe based on the area covered by the form [5], but there is general agreement on this definition or where such areal-based boundaries would lie. Distinguishing between the size of tafoni could be important for identifying if researchers are referring to the same form and by implication the same processes of formation and stabilization, or where changes in the size of the form reflect changes in processes of formation and stabilization [5].

The processes producing tafoni have been postulated as purely physical [14–16], chemical [17,18], biological [8], as well as a mix of process agents [19]. A common thread has been the importance of salt and moisture movements in the formation of the initial pits with a subsequent acceleration of decay rates through variation in external factors, such as evaporation rates, moisture cycles and movement [20–23]. Additionally, positive feedbacks mechanisms within the hollows, such as enhanced salt migration or moisture cycling, have also been viewed as affecting the nature and rates of tafoni development [24,25]. Recent research [26,27] has suggested that tafoni formation could

be viewed through the lens of the increasing constraints imposed by structural, process-based and geometric relations. In particular, rock properties have been viewed as a key controlling factor [26], where different processes, such as freeze-thaw, salt decay and chemical decay, produce the same effect, disassociation of rock, but the nature of the rock itself controls nature of that disassociation. Tafoni development could also be viewed as the outcome of the relations between form and process where form development is canalized or guided along a particular, limited set of pathways [27]. Tafoni development in this conceptual framework is initially constrained by rock structure, but rock structure alone is not sufficient to determine whether tafoni develop or not. Instead rock structure defines the limited or constraining context within which processes operate which then themselves define the constraining context for the development of the internal geometry of the tafoni. This nested hierarchy of constraining factors then provides a basis for understanding how a seemingly diverse set of formative processes result in a convergence of forms as these constraining factors canalize tafoni development.

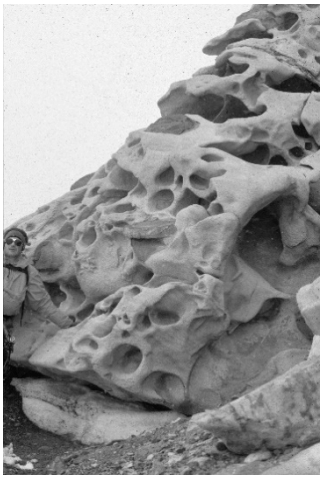

**Figure 1.** Illustration of the tafoni measured.

**Figure 2.** Close-up of some of the tafoni measured. Note the flaked nature of the base of the form suggesting activity rock decay and reduction in the strength of the intact rock.

Viewing tafoni development through such new frameworks suggests that rather than just a visually striking, intellectual curiosity these forms could be used to explore some key issues about forms in nature. Tafoni research has tended to focus on differences in terminology and upon identifying specific processes or agents as formative mechanisms or specific environmental factors as key determinants of tafoni development. If, as recent research suggests [26,27], tafoni represent form convergence through a diversity of processes, then maybe discussions should move from seeking a common set of formative processes to complimentary discussions about the convergent nature of tafoni form. This paper aims to start this discussion by using data collected by the "Landscape Processes in Antarctic Ecosystems" team, to explore how tafoni form can be interpreted within the concepts outlined by recent papers exploring the shape of pebbles [28–31], as well as a recent mathematical model of

tafoni development [32]. Placing the analysis of tafoni shape within this context it is possible to explore how tafoni could develop with only a set of relatively simple and generalized assumptions concerning process-form relationships [32]. Likewise, by focusing only upon how the relationships between simple dimensions of shape change as tafoni enlarge enables the key trends in shape to emerge, and for these trends to be considered without any assumptions concerning specific formative processes.

## 2. Tafoni, Fragments and Shape

Recent papers exploring pebble shape and size and its variation with transportation have begun to converge on a number of similar results. Novak-Szabo et al. [31] used theoretical analysis and simulations to suggest that there are a set of universal characteristics to the evolution of the shape of pebbles by bed-load chipping. The universal characteristics are viewed as the inevitable geometric consequences of brittle fracture. Universality in this sense means the convergence of the details of the system being studied to a similar end point. This means that whatever the initial pebble size and shape, it will, inevitably, tend towards a 'universal' size and shape. It has been suggested that pebble shapes are inevitable because of three key constraints [31]. Firstly, fragments are initially elongated, secondly, particles tend to collide with similar size particles and thirdly, collision energy is relatively small so chipping of the pebble mass dominates over fragmentation. Combined these three constraints mean that attrition by chipping can be modelled as a process of diffusion of surface curvature. This means that the chipping tends to reduce protruding parts of a curve surface first and so whatever the nature of the original surface of the fragment, it will end up as a relatively smooth curved surface.

The shapes of fragments can be explored through experimental analysis of fragmenting by hammering, explosion and weathering [29]. Data on the fragments produced is then used to construct a theoretical model of the development of fragment shape. As in [31], it is suggested that energetic fragmentation processes produce fragments which have an elongated initial form. Previous work on fragmentation, they state, has focused on the statistics of the masses of the fragments produced [33–35] which tend to conform to a power law distribution with the exponent $\tau$ determined by the system dimensionality and, importantly, the brittle and ductile character of the mechanical response of the material. Domokos et al. [28] suggest that analysis of the shape of these fragments reveals a set of universal characteristics for fragments derived from brittle, heterogeneous material whether these fragments are produced by high magnitude, short duration processes, such as explosions or by relatively longer duration processes of cracking through erosion.

Shape was analysed using the length of the fragment, L, and its relationship to the dimensionless ratios (S/L) and (I/L) where S refers to fragment height and I refers to fragment width [5]. Within tafoni terminology, S equates to depth (D) and I equates to width (W). Figure 3 presents an idealized curve of the relationships identified between these ratios and fragment length. The graph shows a clear size dependence of fragment shape with fragment length expressed by the exponential relations:

$$S/L = A_s \exp(-(L - L_c)/L_o) + B_s, \quad (1)$$

$$I/L = A_t \exp(-(L - L_c)/Lo) + B_t, \quad (2)$$

where $L_c$ is the fragment size at which isotropic (uniform) shape is reached, and $L_o$ is the scale parameter that controls how rapidly fragments converge to the shape of the large fragments. Both $L_c$ and $L_o$ are the same value for S and I. $A_s$ and $A_t$ were obtained by best fit, and are 0.45 and 0.4 respectively, so similar values, whilst $B_s$ was 0.43 and $B_t$ was 0.67. Their analysis suggests that once fragments are large enough (i.e., L >> Lc + Lo) then they converge onto an elongated shape where S/L $\approx B_s$ and I/L $\approx B_t$ or S/L $\approx$ 0.43 and I/L $\approx$ 0.67. They explain this convergence through modelling of the fragmentation process which they view as a process of sequential binary breakup beginning with a single cuboid body. Using a stochastic modelling process with a breaking probability of 0.8, fragments either breakup into two pieces of equal mass or they keep their current size [29]. Longer fragments tend to break apart more easily perpendicular to the long axis and this is modelled as a probability function.

The outcome of the modelling process is that above a certain length fragment shape converges to the curves identified from the experimental work.

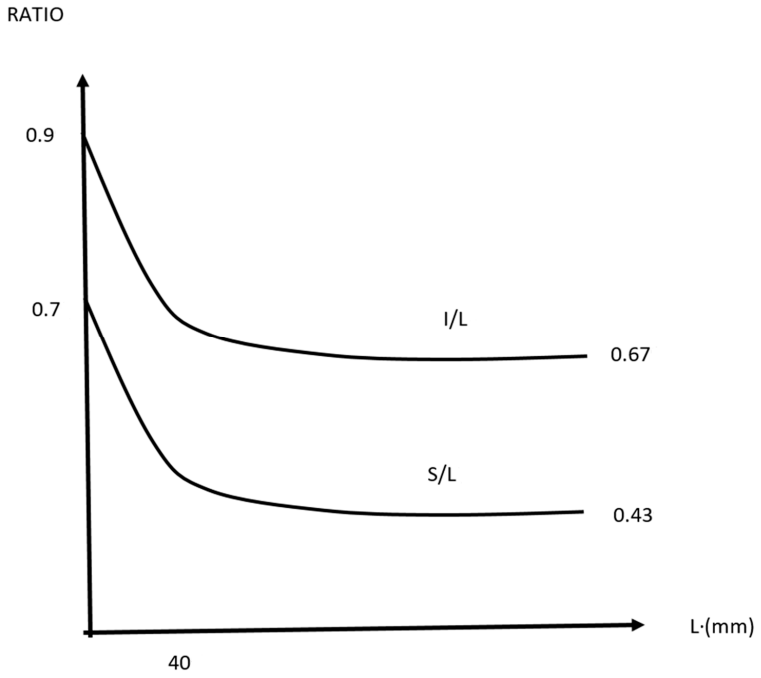


**Figure 3.** Representation of relationship between W/L and D/L ratios and L. (Modified from Domokos, 2015).

The ideas above could be of relevance to tafoni research if the hollow of the tafone are viewed as the other side of the mould from which the fragments originated. It could be assumed that a single fragment produced by a single erosional event would leave a negative mould of its form in the rock face, the size and shape of which would be a mirror image of the fragment. A single tafone is not however the outcome of a single erosional (and transport) event. The shape of a single tafone represents the summation of all the erosional events that have produced it, but whether this results in a convergence on a universal form and the potential relationships of that form to the fragmentation research above is unclear. Such an outcome would highlight that tafone dimensions represent the outcome of the operation of fundamental principles and their relationships that are applicable to the development of such forms in any environment. The convergence to a universal shape would also suggest that tafone development is a process of information loss in the sense that the convergence of form means the loss of information about the origin form of the tafoni. Whatever the original shape of the tafone, evolution of the form will always converge to a specific relationship between the dimensions of the tafone.

A mathematical model of pit evolution has been developed [32] that uses and applies a set of simple rules about the flow and deposition of a corrosion gas, representing salt deposition, and the impact of this corrosive gas on a surface of variable strength. The authors of the model stated that other physical agents can be modelled using a similar framework. In the model pits formed when fluctuations in the corrosion process, in terms of deposition of corrosive particles that then removed discrete, small units of the surface with a specific probability, created depressions. The depressions create a funnel effect that tends to increase the concentration of particles towards the base of the pit, a tendency which is countered by the absorption of particles by the pit walls. The deepening is limited, however, by the development of pits on the rest of the surface and so capture of particles by those pits. This depth limit is an essential outcome of the model and this critical depth identifies pit stability, the point at which other pits will not absorb that pit. Below that depth, pits can coagulate. Widening of a pit occurs from the base of the pit outwards and so erosion is greatest at the base of a pit. The resultant form of the regularly spaced pits in the model is of a collection of trapezoidal pits.

Significantly, the model identified that there were clear and very distinct conditions that were required for pit formation to occur. Specifically, the corrosion probability, $p_c$, the probability for the absorption of a corrosive particle by the surface, needed to be within a specific range. Absorption of a corrosive particle into the surface reduces the surface strength by a fixed amount, so the tuning of this parameter is a key component of the model. This change in rock strength highlights the importance of weathering as a precursor to the removal of material for the formation of the tafoni, but the end form, the tafoni, require an erosional event to develop. The parameter, however, is also relational in the sense that its impact depends not only upon its own value, but upon the strength value of the surface it is absorbed into. If $p_c$ is too high, then pits deepening effect will not occur as particles are not able to sufficiently explore the pit surface and so migrate to the deepest part of the pit before absorption. Similarly, the absence of any initial random variations in surface strength means that all surface sites are destroyed at the same rate and so pits are unable to form. These two terms combine to define the envelope of conditions within which pits could form. An important observation about this model is that, although it deals with discrete erosional events, these are at the scale of individual and identically sized and shaped portions of the surface. Erosion is by removal of small, discrete portions, analogous to small volumes, but relatively continuous erosional loss. The resultant pits are regularly spaced, but also regular in their plan form as having roughly similar lengths and widths.

## 3. Relationships between Shape Indices of Antarctic Tafoni

800 individual tafone dimensions were collected from Antarctica to create a morphospace of tafoni form [27]. The tafoni were measured in Dronning Maud Land, Antarctica in the Austral summers of 2008/09 and 2010/11. The rock in the area is Precambrian in origin and the exposures were of the Borgmassivet Instrusives which is comprised of doleritic and dioritic sills. Measurements of tafoni were made on the nunataks on the Ahlmannryggen (Ahlmann Ridge), more specifically on nunataks, Vesleskarvet (Northern Buttress; 71°40′ S, 2°51′ W), Lorenzenpiggen (71°45′ S, 2°50′ W), Grunehogna (72°02′ S, 2°48′ W), Flarjuven Bluff (72°01′ S, 3°24′ W) and Robertskollen (71°27′ S, 3°15′ W). Measurements were made on 40 rock faces with sampling starting at the central point of each rock face until 10 tafoni had been measured. Tafoni dimensions were measured using a set of callipers and all measurements were made by the same observer to ensure consistency in the field definition of length, width and depth.

A subset of 717 of these tafoni are used to explore the dimensional relationships identified in the above papers. The dimensions of length (L), width (W which was dimension I [29] and depth (D which was dimension S in [29]) were the basis for calculating the ratios of width to length (W/L) and depth to length (D/L). These ratios were selected as they have been used in recent research on fragments shape. Further work could be undertaken on a whole host of shape indices [36], but it was felt those selected provided a good basis for comparing tafone data to the recent fragment research literature. All tafoni with W/L and D/L ratios greater than 1 were excluded from the analysis as these shape indices implied that the dimensions were wrongly defined, or they were clearly the outcome of forms merging. This only amounted to 10% of the original data set. Analysis of relationships used non-parametric statistical analysis of Spearman rank correlation, Kruskal-Wallis test of differences between the median of three or more samples and Mann Whitney U test to assess the difference between two samples. Non-parametric statistics were used in the analysis to avoid the assumptions of normality in the data associated with the use of parametric statistical methods.

Previous research on tafoni has tended to focus on either comparison of data from different sites or environments [7,8,37–39] or on deriving clear linear or curvilinear relationships for tafoni development [21,40–42]. The relatively large size of this data set enabled another approach to be taken to the data in testing how it related to the analysis of fragment shape [29], specifically focusing analysis on the significance of dimensional ratios to fragment length with the resulting convergence of these ratios to specific values as fragment length increased. The tafoni data were divided into quintile (144 values per quintile) and deciles (72 values per decile) and analysis of relationships focused upon

changes within and between these divisions. By grouping tafoni data together in this manner any variability in tafoni dimensions or variations generated by differences in rock strength or other factors at a site would be not distorted attempts to derive relationships between median values for dataset divisions and changes in tafoni length. Variability of individual tafone dimensions would not mask general trends within divisions of the dataset.

Table 1 illustrates the key descriptive statistics for the data set as a whole and then for separate quintiles and deciles. As tafoni length increase both ratios, W/L and D/L do seem to converge, but the apparent value for convergence seems to vary. Kruskal Wallis analysis of the difference between medians across quintiles and deciles (Tables 2 and 3) for dimensions and ratios highlights that, taken as a whole, there are statistically significant differences between median values. Width and depth values increase with each division and the H value does seem to represent a general, significant change in the median value for each division. For the ratios, W/L and D/L the median values do not seem to change in as consistent a manner so the statistically significant H values may reflect key differences between one or two divisions and the rest.

**Table 1.** Statistics of length, width, depth, W/L and D/L ratios for all data, quintiles and decile (all units in cm).

| | **Length** | | **Width** | | **Depth** | | **W/L** | | **D/L** | |
|---|---|---|---|---|---|---|---|---|---|---|
| | *Median* | *Interquartile Range* | *Median* | *Interquartile Range* | *Median* | *Interquartile Range* | *Median* | *Interquartile Range* | *Median* | *Interquartile Range* |
| *All* | 12.80 | 9.32–18.79 | 7.98 | 6.03–12.14 | 5.80 | 4.14–9.12 | 0.67 | 0.54-0.79 | 0.49 | 0.36–0.64 |
| *Quintiles* | | | | | | | | | | |
| $1^{st}$ | 7.21 | 6.11–8.12 | 5.17 | 4.10–6.30 | 3.82 | 3.03–4.69 | 0.75 | 0.65–0.85 | 0.54 | 0.44–0.74 |
| $2^{nd}$ | 9.90 | 9.32–10.40 | 6.52 | 5.42–7.60 | 5.12 | 4.08–6.58 | 0.66 | 0.59–0.77 | 0.51 | 0.41–0.70 |
| $3^{rd}$ | 12.80 | 12.18–13.62 | 8.04 | 6.54–9.76 | 5.58 | 4.52–7.22 | 0.62 | 0.51–0.76 | 0.44 | 0.35–0.58 |
| $4^{th}$ | 17.14 | 15.62–18.78 | 10.92 | 8.90–12.98 | 7.12 | 5.44–10.46 | 0.63 | 0.52–0.75 | 0.42 | 0.30–0.59 |
| $5^{th}$ | 29.77 | 25.00–41.57 | 20.12 | 14.66–27.41 | 16.21 | 14.66–27.41 | 0.65 | 0.48–0.80 | 0.52 | 0.30–0.68 |
| *Deciles* | | | | | | | | | | |
| $1^{st}$ | 6.11 | 5.23–6.84 | 4.19 | 3.62–5.20 | 3.51 | 2.7–4.02 | 0.75 | 0.66–0.84 | 0.57 | 0.47–0.77 |
| $2^{nd}$ | 8.11 | 7.71–8.56 | 6.14 | 5.15–6.82 | 4.17 | 3.40–5.47 | 0.76 | 0.65–0.85 | 0.51 | 0.42–0.71 |
| $3^{rd}$ | 9.32 | 9.02–9.62 | 6.28 | 5.12–7.28 | 4.98 | 3.84–6.32 | 0.67 | 0.56–0.78 | 0.51 | 0.43–0.67 |
| $4^{th}$ | 10.40 | 10.10–10.82 | 6.85 | 5.79–8.07 | 5.33 | 4.11–6.85 | 0.65 | 0.56–0.77 | 0.51 | 0.40–0.67 |
| $5^{th}$ | 12.19 | 11.71–12.52 | 7.34 | 6.29–9.23 | 5.44 | 4.15–7.27 | 0.61 | 0.51–0.78 | 0.46 | 0.35–0.61 |
| $6^{th}$ | 13.62 | 13.10–14.08 | 8.58 | 7.18–10.02 | 5.66 | 4.88–7.16 | 0.63 | 0.51–0.75 | 0.43 | 0.36–0.53 |
| $7^{th}$ | 15.62 | 15.09–16.47 | 10.27 | 7.95–12.13 | 6.90 | 5.39–8.68 | 0.66 | 0.51–0.78 | 0.44 | 0.34–0.56 |
| $8^{th}$ | 18.78 | 17.96–19.56 | 12.12 | 10.00–13.82 | 7.46 | 5.44–11.62 | 0.63 | 0.54–0.74 | 0.41 | 0.29–0.62 |
| $9^{th}$ | 25.00 | 22.74–27.43 | 17.74 | 12.48–20.74 | 12.67 | 7.40–17.49 | 0.69 | 0.51–0.82 | 0.53 | 0.30–0.68 |
| $10^{th}$ | 41.35 | 33.81–61.75 | 27.07 | 19.54–35.84 | 20.79 | 12.53–34.90 | 0.58 | 0.46–0.78 | 0.51 | 0.29–0.65 |

**Table 2.** Statistics for comparison of width, depth, W/L and D/L ratios across quintiles.

| **Quintile** | **Width** | **Depth** | **W/L** | **D/L** |
|---|---|---|---|---|
| $1^{st}$ | 5.17 | 3.82 | 0.75 | 0.54 |
| $2^{nd}$ | 6.52 | 5.12 | 0.66 | 0.51 |
| $3^{rd}$ | 8.04 | 5.58 | 0.62 | 0.44 |
| $4^{th}$ | 10.92 | 7.12 | 0.63 | 0.42 |
| $5^{th}$ | 20.12 | 16.21 | 0.65 | 0.52 |
| *H value* | **498.50** | **340.56** | **46.15** | **38.91** |

*xxx* = statistically significant at $\alpha = 0.05$ **xxx** = statistically significant at $\alpha = 0.01$.

Tables 4 and 5 outline the statistical significance or otherwise of a Mann Whitney U comparison of all potential pairs of quintiles and deciles divisions. This form of analysis allows identification of which quintiles and deciles divisions are statistically significantly different from other quintiles and deciles. For width and depth there is a clear, consistent increase in median value as you move from lower to higher divisions in the quintiles and deciles. For ratios, this consistent pattern is not present. Instead, the lowest quintile and deciles have statistically significantly higher values than the upper quintiles and deciles. These higher quintiles and deciles have median values similar to each

other, except for the highest ones which have slightly, but still significantly higher median values. This suggests that the median value of ratios begins comparatively high and then, relatively rapidly, declines to a lower value that is then, more or less, the same across the the other divisions; a similar pattern to that identified for fragments.

**Table 3.** Statistics for comparison of width, depth, W/L and D/L ratios across deciles.

| Deciles | Width | Depth | W/L | D/L |
|---|---|---|---|---|
| $1^{st}$ | 4.19 | 3.51 | 0.75 | 0.57 |
| $2^{nd}$ | 6.14 | 4.17 | 0.76 | 0.51 |
| $3^{rd}$ | 6.28 | 4.98 | 0.67 | 0.51 |
| $4^{th}$ | 6.85 | 5.33 | 0.65 | 0.51 |
| $5^{th}$ | 7.34 | 5.44 | 0.61 | 0.49 |
| $6^{th}$ | 8.58 | 5.66 | 0.63 | 0.43 |
| $7^{th}$ | 10.27 | 6.90 | 0.66 | 0.44 |
| $8^{th}$ | 12.12 | 7.46 | 0.63 | 0.41 |
| $9^{th}$ | 17.74 | 12.67 | 0.69 | 0.53 |
| $10^{th}$ | 27.07 | 20.79 | 0.58 | 0.51 |
| *H value* | **520.24** | **358.76** | **51.75** | **41.76** |

*xxx* = statistically significant at $\alpha = 0.05$ **xxx** = statistically significant at $\alpha = 0.01$.

**Table 4.** Whitney U test comparison between pairs of quintiles for width, depth, W/L and D/L ratios.

| **Width** | | | | |
|---|---|---|---|---|
| *Quintiles* | $1^{st}$ | $2^{nd}$ | $3^{rd}$ | $4^{th}$ |
| $1^{st}$ | X | | | |
| $2^{nd}$ | S | X | | |
| $3^{rd}$ | S | S | X | |
| $4^{th}$ | S | S | S | X |
| $5^{th}$ | S | S | S | S |
| **Depth** | | | | |
| *Quintiles* | $1^{st}$ | $2^{nd}$ | $3^{rd}$ | $4^{th}$ |
| $1^{st}$ | X | | | |
| $2^{nd}$ | S | X | | |
| $3^{rd}$ | S | S | X | |
| $4^{th}$ | S | S | S | X |
| $5^{th}$ | S | S | S | S |
| **W/L** | | | | |
| *Quintiles* | $1^{st}$ | $2^{nd}$ | $3^{rd}$ | $4^{th}$ |
| $1^{st}$ | X | | | |
| $2^{nd}$ | S | X | | |
| $3^{rd}$ | S | N | X | |
| $4^{th}$ | S | N | N | X |
| $5^{th}$ | S | N | N | N |
| **D/L** | | | | |
| *Quintiles* | $1^{st}$ | $2^{nd}$ | $3^{rd}$ | $4^{th}$ |
| $1^{st}$ | X | | | |
| $2^{nd}$ | N | X | | |
| $3^{rd}$ | S | S | X | |
| $4^{th}$ | S | S | N | X |
| $5^{th}$ | S | N | N | N |

N = Not statistically significant S = Statistically significant at $\alpha = 0.05$.

**Table 5.** Whitney U test comparison between pairs of deciles for width, depth, W/L and D/L ratios.

| **Width** | | | | | | | | | |
|---|---|---|---|---|---|---|---|---|---|
| *Deciles* | $1^{st}$ | $2^{nd}$ | $3^{rd}$ | $4^{th}$ | $5^{th}$ | $6^{th}$ | $7^{th}$ | $8^{th}$ | $9^{th}$ |
| $1^{st}$ | X | | | | | | | | |
| $2^{nd}$ | S | X | | | | | | | |
| $3^{rd}$ | S | S | X | | | | | | |
| $4^{th}$ | S | S | S | X | | | | | |
| $5^{th}$ | S | S | S | S | X | | | | |
| $6^{th}$ | S | S | S | S | S | X | | | |
| $7^{th}$ | S | S | S | S | S | S | X | | |
| $8^{th}$ | S | S | S | S | S | S | S | X | |
| $9^{th}$ | S | S | S | S | S | S | S | S | X |
| $10^{th}$ | S | S | S | S | S | S | S | S | S |
| **Depth** | | | | | | | | | |
| *Deciles* | $1^{st}$ | $2^{nd}$ | $3^{rd}$ | $4^{th}$ | $5^{th}$ | $6^{th}$ | $7^{th}$ | $8^{th}$ | $9^{th}$ |
| $1^{st}$ | X | | | | | | | | |
| $2^{nd}$ | S | X | | | | | | | |
| $3^{rd}$ | S | N | X | | | | | | |
| $4^{th}$ | S | S | N | X | | | | | |
| $5^{th}$ | S | S | S | N | X | | | | |
| $6^{th}$ | S | S | S | N | N | X | | | |
| $7^{th}$ | S | S | S | S | S | S | X | | |
| $8^{th}$ | S | S | S | S | S | S | N | X | |
| $9^{th}$ | S | S | S | S | S | S | S | S | X |
| $10^{th}$ | S | S | S | S | S | S | S | S | S |
| **W/L** | | | | | | | | | |
| *Deciles* | $1^{st}$ | $2^{nd}$ | $3^{rd}$ | $4^{th}$ | $5^{th}$ | $6^{th}$ | $7^{th}$ | $8^{th}$ | $9^{th}$ |
| $1^{st}$ | X | | | | | | | | |
| $2^{nd}$ | N | X | | | | | | | |
| $3^{rd}$ | S | S | X | | | | | | |
| $4^{th}$ | S | S | N | X | | | | | |
| $5^{th}$ | S | S | N | N | X | | | | |
| $6^{th}$ | S | S | N | N | N | X | | | |
| $7^{th}$ | S | S | N | N | N | N | X | | |
| $8^{th}$ | S | S | N | N | N | N | N | X | |
| $9^{th}$ | S | S | N | N | N | N | N | N | X |
| $10^{th}$ | S | S | S | N | N | N | N | N | N |
| **D/L** | | | | | | | | | |
| *Deciles* | $1^{st}$ | $2^{nd}$ | $3^{rd}$ | $4^{th}$ | $5^{th}$ | $6^{th}$ | $7^{th}$ | $8^{th}$ | $9^{th}$ |
| $1^{st}$ | X | | | | | | | | |
| $2^{nd}$ | N | X | | | | | | | |
| $3^{rd}$ | N | N | X | | | | | | |
| $4^{th}$ | S | N | N | X | | | | | |
| $5^{th}$ | S | S | N | N | X | | | | |
| $6^{th}$ | S | S | S | S | N | X | | | |
| $7^{th}$ | S | S | S | S | N | N | X | | |
| $8^{th}$ | S | S | S | S | N | N | N | X | |
| $9^{th}$ | S | N | N | N | N | N | N | N | X |
| $10^{th}$ | S | S | N | N | N | N | N | N | N |

N = Not statistically significant; S = Statistically significant at $\alpha = 0.05$.

Within each division there were sufficient data points to permit an analysis of how dimensions and ratios were correlated to length (Table 6). Across the dataset as a whole there was a statistically significant negative correlation between length and width and length. This significant correlation

was repeated for the lowest and highest divisions, but only occurred occasionally across all other divisions. Similarly, the correlation coefficient for W/L to length and D/L to length was statistically significant for the data set as a whole and for the lowest and highest divisions, but not usually for divisions in between. This suggests that ratios are only statistically significantly correlated with length for relatively small tafone and once beyond a certain size there is stability in these ratios that are not affected by increasing the size of the tafoni lengthwise.

**Table 6.** Rank correlation analysis of the association between length and width, depth, W/L and D/L ratios for the whole dataset, for each quintile and for each decile.

| | **Width** | **Depth** | **W/L** | **D/L** |
|---|---|---|---|---|
| *All* | **0.851** | **0.698** | **−0.161** | *−0.093* |
| *Quintiles* | | | | |
| $1^{st}$ | **0.663** | **0.364** | −0.031 | **−0.232** |
| $2^{nd}$ | **0.245** | *0.193* | −0.031 | 0.031 |
| $3^{rd}$ | 0.144 | 0.125 | −0.109 | −0.073 |
| $4^{th}$ | **0.348** | 0.106 | −0.006 | −0.015 |
| $5^{th}$ | **0.419** | **0.410** | **−0.216** | −0.028 |
| *Deciles* | | | | |
| $1^{st}$ | **0.650** | 0.146 | −0.032 | **−0.390** |
| $2^{nd}$ | *0.239* | 0.057 | −0.108 | −0.119 |
| $3^{rd}$ | *0.288* | 0.164 | 0.134 | 0.083 |
| $4^{th}$ | 0.072 | 0.198 | −0.072 | 0.105 |
| $5^{th}$ | −0.120 | 0.071 | −0.214 | −0.050 |
| $6^{th}$ | −0.005 | 0.072 | −0.140 | −0.029 |
| $7^{th}$ | 0.219 | 0.005 | 0.092 | −0.107 |
| $8^{th}$ | **0.309** | 0.025 | 0.105 | 0.080 |
| $9^{th}$ | 0.090 | 0.191 | −0.040 | 0.138 |
| $10^{th}$ | **0.339** | **0.366** | *−0.265* | −0.035 |

*xxx* = Statistically significant at $\alpha = 0.05$; **xxx** = Statistically significant at $\alpha = 0.01$.

## 4. Discussion

From the above analysis it is possible to begin to interpret tafoni within the context of the mathematical model of tafoni development [32] and fragment shape research [29]. The relationship between length and ratios does seem to mirror the observations from recent research [29] in that initially comparative high values for ratio seem to then converge onto a specific value. The values hover around 0.62 to 0.66 for W/L and around 0.44 to 0.50 for W/D, although the values for the latter ratio is more variable than the values for the W/L ratios. The convergence values are remarkably similar to those in Figure 1, i.e., 0.67 for W/L and 0.43 to D/L ratios. This could suggest that tafoni do reflect, to some extent, the brittle fracture fragmentation processes. This research, however, is concerned with fragments rather than the mould those fragments leave behind. As noted above, tafoni shape will reflect multiple erosional events, large and small, rather than a single large erosional event. Certainly, development of tafoni of increasing size could not be attributed to a single event, so tafoni shape needs to be interpreted in relation to multiple events that seem to maintain a shape that seems to still conform to the findings concerning fragment shape.

The mathematical model of tafoni development [32] shows how a simple set of rules about the relationships between a surface of variable strength and the action of aggressive erosional agents can produce a regular lattice of trapezoidal forms that are limited in depth through their interactions. Repeated small volume erosional processes produce, under highly constrained conditions, a surface where regularly spaced pits can form. Although this research did not include any measurement of dimensions, the lattices produced suggest a length to width ratio of approximately 1:1.

Combing insights from the research above might suggest that tafone shape reflects both the operation of small volume and virtually continuous erosional processes, as well as the shaping, beyond a critical length, from fragmentation processes. Modelling offers a mathematically based explanation as to why regularly spaced groups of tafone might develop on the surface in the first place. The definition of key constraining conditions will limit potential tafone development to only certain types of rock surface where the relationships between rock strength and aggressive erosional agents, as manifest in the corrosion probability, matches the model's conditions. On such surfaces, tafoni will develop whose size depends on the specific conditions of this relationship. The model suggests that such forms will have all have a common, limited depth based on this relationship. In plan, these forms will tend to be trapezoidal and so have a comparatively high W/L ratio.

As tafoni grow in size, however, there is increasing likelihood that large volume fragmentation or fracturing events will also occur within and around them. Weakening the structure of the rock through the creation of cavities, particularly at the edges of the pit, will mean that fracturing and fragmentation are likely to be an edge-based erosional process and also the location where fragments will be generated. This implies that as the pits widen there is an increase in the likelihood that large fractures and fragments will be produced, and therefore, such fragments will increasingly conform to the W/L ratios identified [29]. The mould of such singular fragments will be preserved in an individual tafone. In addition, the smaller volume, shorter duration processes, identified in the mathematical model [32] would still be operating on the new surface, the mould left by the fragment. These processes would produce a smoothing affect analogous to chipping mentioned above.

The ratio data seems to suggest that as tafoni lengthen the ratios remain roughly the same. This would suggest that fragmentation and its dimensions increasingly dominate the shape of tafone. Indeed, the data might imply that as tafoni lengthen then larger fragmentation events become increasingly important to the shape of the tafone with singular large events dictating the overall shape of the form which is then only slightly modified by smaller volume erosional events. Fragmentation adds another process that increases tafone size and so adds another potential way that tafoni can compete for space on the rock surface. As the initial development of tafone was as a set of regularly-spaced features then this is the format within which fragmentation occurs. It is likely that regularity of spacing will be maintained if fragmentation processes occur with equal probability across a surface as merging of tafoni expanding at similar rates interact. If fragmentation occurs with a differential probability across the surface, then it is likely that tafoni will expand at different rates and so a size-frequency distribution of tafone will develop that reflects this differential rate.

Initial development of tafoni is dominated by the relationships between relatively small spatial variations in rock strength, the concentration of erosional agents and the corrosive probability function. Once initiated the positive feedback generated through the funnel effect of a pit focuses erosion in the pit base, the depth of which is limited through the interaction with other pits on the surface. Pits then widen though erosion at the pit base. The resulting regularly-spaced forms are generally trapezoidal in shape with a length to width ratio of roughly 1:1. As these forms enlarge then the forms themselves weaken the rock particularly at their edges and so become the focus for fragment production. As the size of the tafoni increases, the fragments produced are increasingly likely to conform to the shape characteristics identified [29]. Even though tafoni shape is not necessarily the product of a single fragmentation event, as size increases so will the size of these events and so it is likely that the overall shape of the tafoni will come to be dominated by such singular event. If this is the case, then the W/L ratio in particular is likely to tend towards the ratio for fragments.

## 5. Conclusions

Tafoni dimensions change with the size of the tafoni, as tafoni become longer, their widths increase and, to a much lesser extent so do their depths. Dimensional ratios, such as W/L and D/L, have a different relationship to length. As tafoni increase in length, these ratios converge on a particular value of about 0.65 for W/L and about 0.45 for D/L. Recent research in mathematically modelling

tafoni development and in the analysis of fragment size and shape suggest that there may be a physical basis to this convergence. Initial development of tafoni can be explained within the mathematical model which simulates tafoni development as the outcome of the interaction between variable rock strength, concentration variations of corrosive agents and the corrosive probability function. Combined these parameters result in a regularly-spaced set of trapezoidal forms with a depth controlled and limited by interaction between pits. The length to width ratio of these features is approximately 1:1. Recent research [29] discusses how fragment shape varies with fragment size and how the ratios of width to length (W/L) and depth to length (D/L) converge on specific values as fragment size increases. The convergent values of 0.67 for width to length and 0.43 for depth to length are very similar to the ratio values found in real tafoni in Antarctica. This suggests that there could be a process connection between these observations. A fragment will leave behind an impression or mould of its form on the rock it is derived from. As tafoni develop there are likely to weaken the rock, particularly at the edge of their depressions. These could become loci for fracturing and fragmentation. Single erosional events could increasingly dominate the shape of a tafone as the fragments increase in size, as the tafone itself does. Although the smaller volume and more continuous erosion identified in the mathematical model will continue to operate and will tend to smooth the surface of the tafoni, the overall shape could increasingly be defined by a few, large fragmentation events. If this is the case, then the dimensional ratios of tafoni will converge towards the values for fragments identified.

This observation of the convergence of ratios is, however, only tested for this dataset, albeit a relatively large dataset, of tafoni dimensions. It will be interesting to see if extending this form of analysis of other datasets for tafoni from different environments and for different rock types produces a convergence to the same ratios or if these ratios are environment or geology dependent.

**Author Contributions:** Writing—original draft, R.I. and K.H.; Writing—review and editing, R.I. and K.H.

**Funding:** This research was funded by the South African National Research Foundation through the South African National Antarctic programme.

**Acknowledgments:** Tafoni data were provided by Ian Meiklejohn, Christel Hansen, Michael Loubser and Werner Nel of the South African "Landscape Processes in Antarctic Ecosystems" project. The authors would like to thank the two reviewers for their constructive criticism.

**Conflicts of Interest:** The authors declare no conflict of interest.

## References

1. Batrum, J.A. Honeycomb weathering of rocks near the shore-line. *N. Z. J. Sci. Technol.* **1936**, *18*, 593–600.
2. Blackwelder, E. Cavernous rock surfaces of the desert. *Am. J. Sci.* **1929**, *17*, 393–399. [CrossRef]
3. Bryan, K. Niches and other cavities in sandstone at Chaco Canyon, New Mexico. *Zeitschrift für Geomorphologie* **1928**, *3*, 125–140.
4. Palmer, H.S.; Powers, H.A. Pits in coastal pahoehoe lavas controlled by gas bubbles. *J. Geol.* **1935**, *43*, 639–643. [CrossRef]
5. Groom, K.M.; Allen, C.D.; Mol, L.; Paradise, T.R.; Hall, K. Defining tafoni: Re-examining terminological ambiguity for cavernous rock decay phenomena. *Prog. Phys. Geogr.* **2015**, *39*, 775–793. [CrossRef]
6. Doehne, E. Salt weathering: A selective review. In *Natural Stone, Weathering Phenomena, Conservation Strategies and Case Studies*; Siegesmund, S., Weiss, T., Vollbreacht, A., Eds.; Special Publications, 205; Geological Society: London, UK, 2002; pp. 51–64.
7. Rodriguez-Navaro, C. Evidence of honeycomb weathering on Mars. *Geophys. Res. Lett.* **1990**, *25*, 3249–3252. [CrossRef]
8. Andre, M.F.; Hall, K. Honeycomb development on Alexander Island, glacial history of George VI sound and palaeoclimatic implications (Two Step Cliffs/Mars Oasis, W Antarctica). *Geomorphology* **2005**, *65*, 117–138. [CrossRef]
9. Siedel, H. *Alveolar Weathering of Cretaceous Building Sandstone on Monuments in Saxony, Germany*; Special Publication 333; Geological Society: London, UK, 2010; pp. 11–23.

10. Turkington, A.V.; Phillips, J.D. Cavernous weathering, dynamical instability and self-organisation. *Earth Surf. Process. Landf.* **2004**, *29*, 665–675. [CrossRef]
11. Dragovich, D. The origin of cavernous surfaces (tafoni) in granitic rocks of southern South Australia. *Zeitschrift für Geomorphologie* **1967**, *13*, 163–181.
12. Gill, E.D. Rapid honeycomb weathering (tafoni formation) in Greywacke, S.E. Australia. *Earth Surf. Process. Landf.* **1981**, *6*, 81–83. [CrossRef]
13. Prebble, M.M. Cavernous weathering in the Taylor dry valley, Victoria land, Antarctica. *Nature* **1967**, *216*, 1194–1195. [CrossRef]
14. Mottershead, D.N.; Pye, K. Tafoni on coastal slopes, south Devon, UK. *Earth Surf. Process. Landf.* **1994**, *19*, 543–563. [CrossRef]
15. Bradley, W.C.; Hutton, J.T.; Twidale, C.R. Role of salts in development of granitic tafoni. *South Aust. J. Geol.* **1978**, *86*, 647–654.
16. Rodriguez-Navarro, C.; Doehne, E.; Sebastian, E. Origins of honeycomb weathering: The role of salts and wind. *Geol. Soc. Am. Bull.* **1999**, *111*, 1250–1255. [CrossRef]
17. Campbell, S.W. Chemical weathering associated with tafoni at Papago Park, central Arizona. *Earth Surf. Process. Landf.* **1999**, *24*, 271–278. [CrossRef]
18. Ietto, F.; Perri, F.; Filomena, L. Weathering processes in volcanic tuff rocks of the "Rupe di Coroglio" (Naples, southern Italy): Erosion-rate estimation and weathering forms. *Rend. Online Soc. Geol. Ital.* **2015**, *33*, 53–56. [CrossRef]
19. Martini, I.P. Tafoni weathering, with examples from Tuscany, Italy. *Zeitschrift für Geomorphologie* **1978**, *22*, 44–67.
20. McBride, E.F.; Picard, M.D. Origin of honeycomb and related weathering forms in Oligocene Macigno sandstone, Tuscan coast near Livorno, Italy. *Earth Surf. Process. Landf.* **2004**, *29*, 713–735. [CrossRef]
21. Huinink, H.P.; Pel, L.; Kopinga, K. Simulating the growth of tafoni. *Earth Surf. Process. Landf.* **2004**, *29*, 1225–1233. [CrossRef]
22. Ietto, F.; Perri, D.; Miriello, S.A.; Ruffolo, A.; Lagana Le Pera, E. Epoxy resin for the slope consolidation intervention on the Tropea sandstone cliff (southern Calabria, Italy). *Geoheritage* **2018**, *10*, 287–300. [CrossRef]
23. Conca, J.L.; Astor, A.M. Capillary moisture flow and the origin of cavernous weathering in dolerites of Bull Pass, Antarctica. *Geology* **1987**, *93*, 59–73. [CrossRef]
24. Mol, L.; Viles, H.A. The rock of rock surface hardness and internal moisture in tafoni development in sandstone. *Earth Surf. Process. Landf.* **2012**, *37*, 301–314. [CrossRef]
25. Mol, L.; Viles, H.A. Geoelectric investigations into sandstone moisture regimes: Implications for rock weathering and the deterioration of san rock art in the Golden Gate reserve, South Africa. *Geomorphology* **2010**, *118*, 280–287. [CrossRef]
26. Hall, K.; Thorn, C.; Sumner, P. On the persistence of 'weathering'. *Geomorphology* **2012**, *149*, 1–10. [CrossRef]
27. Inkpen, R.; Hall, K. Using morphspaces to understand tafoni development. *Geomorphology* **2015**, *261*, 193–199. [CrossRef]
28. Domokos, G.; Jerolmack, D.J.; Sipos, A.A.; Torok, A. How river rocks round: Resolving the shape-size paradox. *PLoS ONE* **2014**, *2*, e88657. [CrossRef] [PubMed]
29. Domokos, G. Universality of fragment shapes. *Sci. Rep.* **2015**, *5*, 9147. [CrossRef] [PubMed]
30. Domokos, G. Natural numbers, natural shapes. *Axiomathes* **2018**. [CrossRef]
31. Novak-Szabo, T.; Sipos, A.A.; Shaw, S.; Bertoni, D.; Pozzebon, A.; Grottoli, E.; Sarti, G.; Ciavola, P.; Domokos, G.; Jerolmack, D.J. Universal characteristics of particle shape evolution by bed-load chipping. *Sci. Adv.* **2018**, *4*, eaa04946. [CrossRef] [PubMed]
32. Burridge, J.; Inkpen, R. Formation and arrangement of pits by a corrosion gas. *Phys. Rev.* **2015**, *91*, 022403.
33. Grady, D.E. Particle size statistics in dynamic fragmentation. *J. Appl. Phys.* **1990**, *68*, 6099–6105. [CrossRef]
34. Astrom, J. Statistical models of brittle fragmentation. *Adv. Phys.* **2006**, *55*, 247–278. [CrossRef]
35. Wittel, F.K.; Kun, F.; Herrmann, H.J.; Kroplin, B.H.; Maloy, K.J. Scaling behaviour of fragment shapes. *Phys. Rev. Lett.* **2006**, *96*, 025504.
36. Blott, S.J.; Pye, K. Particle shape: A review and new methods of characterization and classification. *Sedimentology* **2008**, *55*, 31–63. [CrossRef]
37. Paradise, T.R. Sandstone weathering and aspect in Petra, Jordan. *Zeitschrift für Geomorphologie* **2002**, *46*, 1–18. [CrossRef]

38. Turkington, A.; Paradise, T.R. Sandstone weathering: A century of progress and innovation. *Geomorphology* **2005**, *67*, 229–253. [CrossRef]
39. Paradise, T.R. Assessment of tafoni distribution and environmental factors on a sandstone djinn block above Petra, Jordan. *Appl. Geogr.* **2013**, *42*, 176–185. [CrossRef]
40. Matsukura, Y.; Matsuoka, N. Rates of tafoni weathering on uplifted shore platforms in Nojimazaki, Boso Peninsula, Japan. *Earth Surf. Process. Landf.* **1991**, *16*, 51–56. [CrossRef]
41. Norwick, S.A.; Dexter, L.R. Rates of development of tafoni in the Moenkopi and Kaibab formations in Meteor Crater and on the Colorado Plateau, Northeastern Arizona. *Earth Surf. Process. Landf.* **2002**, *27*, 11–26. [CrossRef]
42. Sunamura, T.; Hisashi, A. Application of an S shaped curve model to the temporal development of tafoni of salt weathering origin. *Earth Surf. Process. Landf.* **2011**, *36*, 1624–1631. [CrossRef]